# Effect of Specimen Geometry on J-resistance Curves in Near Small-scale Yielding Conditions

G. ROUSSELIER, G. DEVESA and M. BETHMONT
*Electricité de France, Service Réacteurs Nucléaires et Echangeurs, Les Renardières, BP 1, F-77250 Moret/Loing, France*

**ABSTRACT**

This paper is dealing with the effect of specimen geometry on $J_R$-curves. A continuum damage mechanics model is used to simulate the crack initiation and growth in a thermally aged cast austenitic stainless steel. The model parameters are calibrated from notched tension specimens and CT specimens $J_R$-curves computed from CT, SECP and CCP specimens are compared.

**KEYWORDS**

Size effect, $J_R$-curves, local approach of fracture, damage model, cast austenitic stainless steel.

**INTRODUCTION**

The effect of specimen geometry on $J_R$-curves is well known. Many experimental results show that $J_R$-curves may depend on the specimen thickness and width, and on the type of loading (tension or bending) - see Garwood, 1982 ; Roos et al. 1987 ; for example. The lower $J_R$-curves are obtained with compact tension (CT) specimens and the steeper with centre cracked panels (CCP). Side grooving of test specimens, eliminating the surface shear lip effects, reduces the slope of the resistance curve and gives "plane strain" mode resistance curves. If generally side grooving tends to diminish the difference between experimental CT and CCP $J_R$-curves, it does not eliminate it totally.

Relatively to the specimen sizes, criteria have been proposed (Mc Mecking and Parks, 1979), as limits in which J is assumed to be independent of the specimen geometry. These criteria are expressed as following : $b > N\ (J/\sigma_o)$ where b is the size of the uncracked ligament, $\sigma_o$ the yield strength and N a nondimensional factor. N has been evaluated from numerical analysis and experimental results. N = 20 or 25 is admitted for CT specimens. Nevertheless, these size requirements are only indicative.

Recently, Mudry et al. (1986) developed a more rigourous analysis based on local approach of fracture, to quantify the J dependency with specimen geometry. The local ductile fracture criterion is based on the physical mechanisms of cavity growth. The damage variable R is calculated at the crack tip with a relation similar to Rice and Tracey's (1969) : $R = l_c \int 0{,}283 \exp (3\,\sigma_m/2\,\sigma_{eq})\, d\varepsilon^p_{eq}$ where $\sigma_m$ is the hydrostatic stress, $\sigma_{eq}$ the equivalent von Mises stress and $l_c$ a microscopic dimension characteristic of the material. The crack is assumed to initiate when R is equal to $R_c$ a critical parameter evaluated from experiments involving notched tensile bars.

The parameters R and J are computed for CT and CCP specimens and compared (Fig. 1). It appears clearly that for a given R value J is higher with the CCP specimens. A noticeable result is that J does not only depend on the relative dimension of crack a/W but also on the strain hardening of the material. These effects of material and specimen geometry are observed for large scale yielding conditions (Mudry et al., 1986).

Can these effects be also encountered even in near small scale yielding conditions, if particular materials of low toughness and high strain hardening coefficient are tested ?

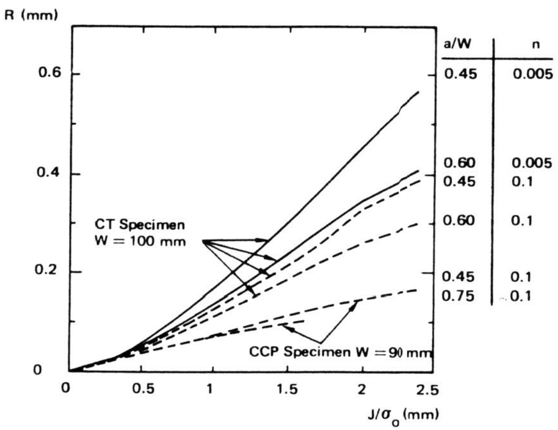


Fig. 1 — Comparison of J parameter and the ductile fracture local criterion R [4] (W : width, n : hardening exponent).

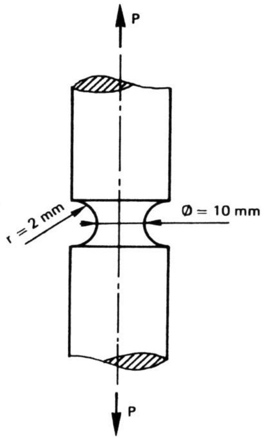


Fig. 2 — Cylindrical notched tensile specimen for calibration of local approach of fracture parameters.



In view to answer to this question a numerical and experimental study is in the making. The first numerical results are given in this paper. Several specimen configurations were analyzed and crack initiation and growth was simulated by local approach fracture based on the damage model developped by Rousselier (1986).

## THE DUCTILE FRACTURE MODEL

The continuum damage mechanics model developed by Rousselier (1986, 1987) was used. On the microscopic level, this model refers to a void growth formula similar to well known Rice and Tracey's (1969). Ductile fracture is included in the plastic constitutive relations through a damage variable β.

The model involves three material parameters to be calibrated :
- $f_o$, initial void volume fraction,
- $\sigma_1$, a stress expressing the fracture resistance of the matrix material (shear resistance, microvoid growth and coalescence, etc ...),
- $l_c$, a characteristic length expressing the interaction between a crack tip and voids. The parameter $l_c$ is not included in the equations of the model ; in numerical applications $l_c$ is the size of the finite elements at the crack tip and does not affect the results when there is no crack, like in notched specimens.

Usually the parameters $\sigma_1$ and $l_c$ are calibrated with mechanical testing of circumferentially notched tensile specimens (Fig. 2). The calibration is achieved when a good agreement is obtained between the experimental and numerical curves. Note that the true stress-strain curve of the material, given by smooth tensile tests, can be checked, extrapolated and if necessary corrected with the notched tensile test data.

Generally, an abrupt change of the curve slope indicates crack initiation in the center of the specimen, and the slope of the curve beyond this point depends on $l_c$ which may be calibrated as $\sigma_1$, by comparison of numerical and experimental results. For the steel tested here, $l_c$ had to be calibrated by comparison with CT specimen $J_R$-curves because the crack initiation point is not well defined on the tensile curve of the notched specimens.

## MATERIAL CHARACTERIZATION

The material tested here is an experimental cast austenitic stainless steel, containing a high ferrite content (more than 30 %). After thermal aging, the damage of this duplex steel may be roughly described in three stages. First the cleavage takes place in ferrite phase at a very small deformation, secondly the microcracks turn into rounded voids, then the final ductile fracture is controlled by the resistance of the austenitic matrix.

The steel was tested at 320°C and the analyses were performed with the material characteristics at the same temperature. The experimental stress- strain curve is directly used in calculations. The extrapolated law including deformation higher than 12 % is expressed as $\sigma = k\ (\varepsilon^{p})^{n}$ with k = 1238 MPa and n = 0.236. The true yield stress is $\sigma_o$ = 128 MPa and Young's modulus is 160 000 MPa. From notched tensile specimen tests the damage model parameters have been evaluated to $f_o = 4.10^{-3}$ and $\sigma_1$ = 200 MPa (Fig. 3). From CT specimen test results, $l_c$ was evaluated equal to 0.55 mm (Fig. 4 and Fig. 5). $l_c$ = 0,55 mm is the best fit with experimental points of Fig. 5. The minimum fracture toughness can be approximated to $J_{IC}$ = 25 kJ/m$^2$.

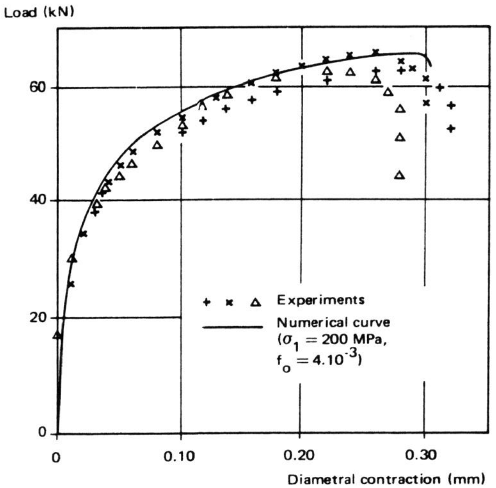


Fig. 3 – Load-displacement curve of cylindical notched tensile specimens.



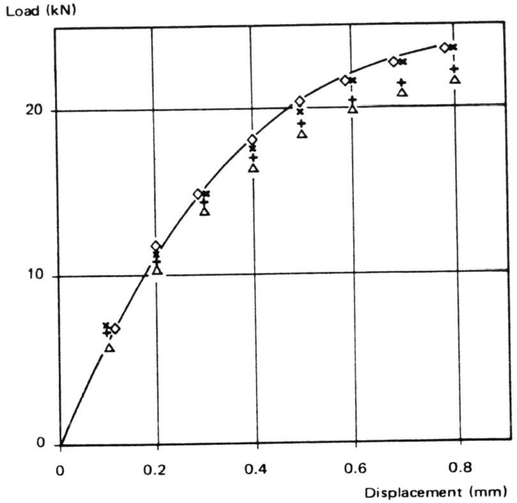


Fig. 4 – Calculated load-displacement curve of the CT specimen and experimental results (4 tests). Thickness = 20 mm.

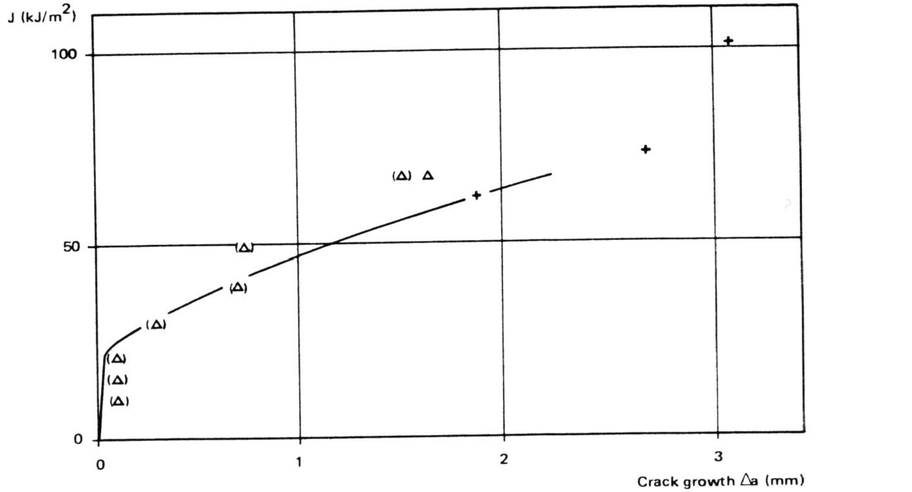


Fig. 5 – Calculated $J_R$ curve of a CT specimen with the damage model ($\sigma_1$ = 200 MPa, $f_o$ = 4.10$^{-3}$ and $\ell_c$ = 0.55 mm) and experimental results :

$\Delta$, + = interrupted test measurements,

($\Delta$) = calculated crack growth from specimen compliance.

## NUMERICAL ANALYSIS OF THE EFFECT OF SPECIMEN GEOMETRY

The numerical analyses were carried out with ALIBABA, a 2D-mechanics finite element program developed by Electricité de France. The geometry changes are taken into account with an updated lagrangian scheme. Non linearities are solved with an implicit algorithm. Calculations were made with 2D plane deformation hypothesis. The finite elements are mostly isoparametric 8-nodes quadrangles with 4 Gauss integration points. The finite element size at the crack tip is $l_c$ = 0.55 mm.

Fig. 6 shows the three specimen configurations to be compared : a CT specimen (previously analyzed to evaluate $l_c$ parameter), a CCP specimen and a Single Edge Cracked Panel (SECP) under remote uniform stress or remote uniform displacement. SECP specimens of two different sizes were analyzed as described in Fig. 6.

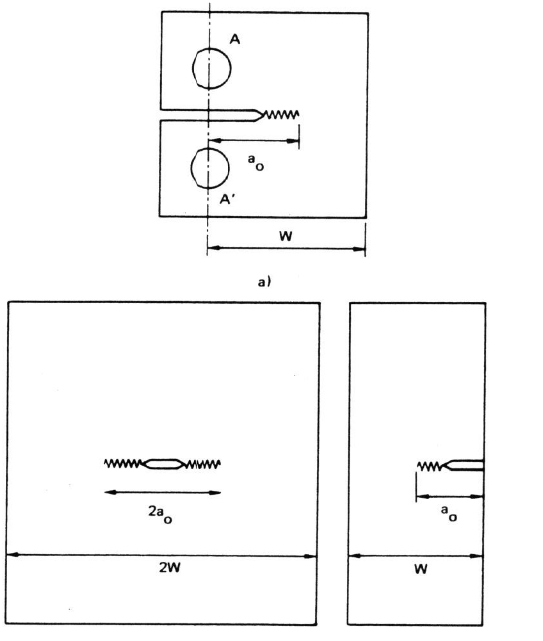


Fig. 6 – Specimen configurations :
a) CT (W = 50 ; $a_o$ = 30 mm),
b) CCP (W = 100 ; $a_o$ = 25 mm),
c) SECP (1) W = 80 ; $a_o$ = 10 mm,
(2) W = 40 ; $a_o$ = 25 mm (remote uniform stress),
(3) W = 40 ; $a_o$ = 25 mm (remote uniform displacement)



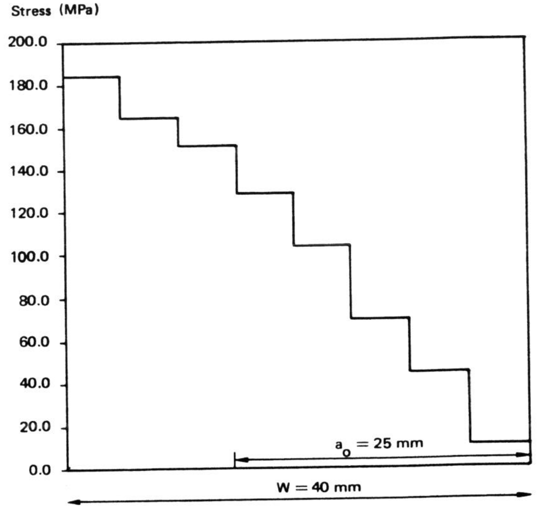


Fig. 7 – Stress distribution at the end of the SECP specimen if remote uniform displacement is applied (W = 40 ; $a_o$ = 25 mm).

The profile of the remote stress through the SECP specimen width depends on boundary conditions if $a_o/b$ = 0.625 ($a_o$ = 25 mm, b = 40 mm) : see Fig. 7. On the other hand, if $a_o/b$ = 0.125 ($a_o$ = 10 mm, b = 100 mm) no influence of boundary conditions can be observed : in the two cases, the stresses are constant through the width. Boundary condition influence is directly observable on the diagram of the load versus crack mouth opening (Fig. 8). The specimen stiffness is higher if remote uniform displacement is applied.

In continuum damage model, stable crack growth comes out as a highly damaged zone. No special techniques like node release or node shifting are needed (Rousselier et al., 1986). When the material surrounding a corner node on the crack line fails, there is an abrupt increase of damage at the next integration point and a corresponding decrease of the stress at the same point.

The $J_R$-curves computed from each specimen are shown in Fig. 9. As described previously the crack growth is calculated from the variation of local stress and damage. The total crack growth $\Delta a$ includes the half-crack tip opening displacement at crack growth initiation, about 0.05 mm, which represents the strech zone generally included in fractographic crack growth measurements. J is

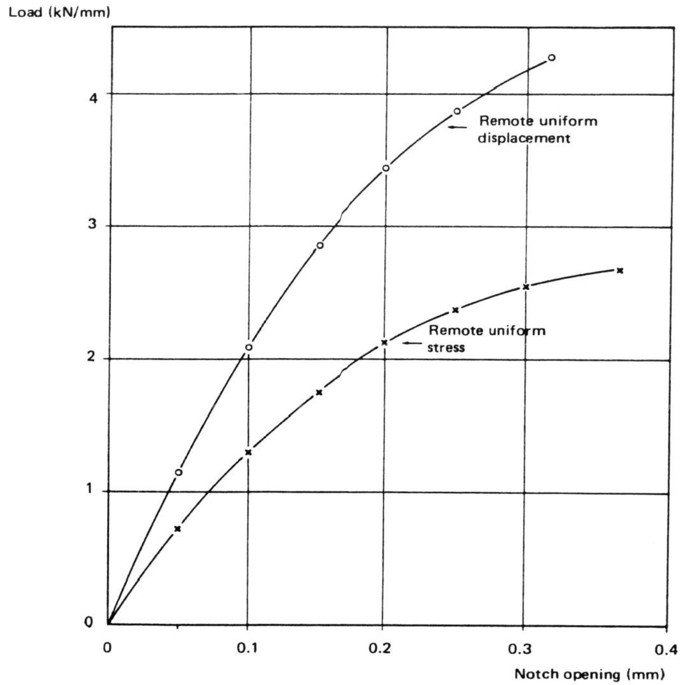


Fig. 8 — Load-displacement (notch opening) curves of the SECP specimen with remote uniform displacement or stress applied at the ends of the specimen. (W = 40 ; $a_o$ = 25 mm).

directly calculated as the path independent integral. It was verified that J values calculated from EPRI method (Kumar et al., 1981) are very close to J-integral.

Fig. 9 shows that the CT specimen J resistance curve is the lowest one. This curve is generally used to characterize the ductile fracture resistance of materials (ASTM E813-81). It can be observed that the increasing of $J_R$ curves corresponds to a decreasing of the bending moment through the uncracked ligament. A margin of 100 % is obtained between the lower (CT) and the higher (CCP) values. The variations of $J_R$ curves were expected ; but the unusual result of this numerical analysis is to point out $J_{IC}$ (crack initiation) specimen geometry dependence for this low toughness material in near small yielding conditions : 25 $(J_{IC}/\sigma_o)$ is smaller than 5 mm-.



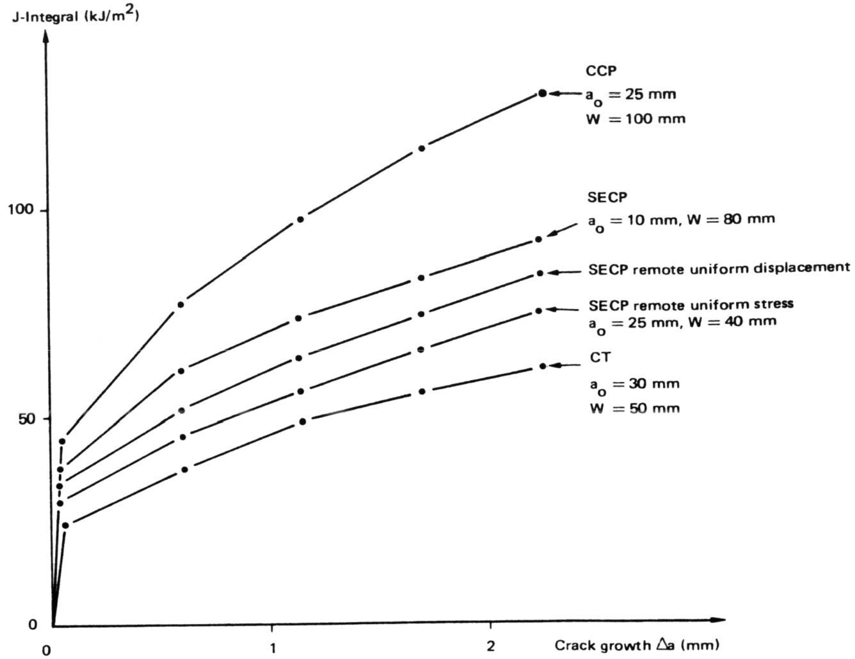


Fig. 9 — Effect of specimen geometry on calculated $J_R$ curve with ductile fracture damage model ($\sigma_1$ = 200 MPa, $f_o = 4.10^{-3}$, $\ell_c$ = 0.55 mm).

## CONCLUSION

A continuum damage mechanics model was used in the frame of local approach of ductile fracture to simulate the crack initiation and growth in a thermally aged cast austeno-ferritic steel with low $J_{IC}$ fracture toughness and high strain hardening. The model parameters were calibrated from notched tension specimens and CT specimens.

Several specimen configurations were analyzed. The numerical results with crack growth simulation point out the great effect of the geometry on J-resistance curves, despite the near small scale yielding conditions.

## REFERENCES


ASTM E 813-81. Standard test for $J_{IC}$, a measure of fracture toughness. Annual book of Standards part 10.

Garwood S.J. (1982). Geometry and orientation effects on ductile crack growth resistance. Int. J. Pres. Ves. and Piping, 10, 297-319.

Kumar V., M.D. German, C.F. Shih (1981). An Engineering Approach for Elastic Plastic Fracture Analysis". EPRI Topical Report NP-1931.

Mc Meeking R.M., and D.M. Parks (1979). In Elastic-Plastic Fracture, ASTM STP 668, 175-194.

Mudry F., F. di Rienzo and A. Pineau (1986). Numerical comparison of global and local fracture criteria in CT and CCP specimens. ASTM Third Non linear Fracture Mechanics Symposium, Knoxville, 6-8 October.

Rice J.R., D.M. Tracey (1969). On the ductile enlargement of voids in triaxial stress fields". J. Mech. Phys. Solids, 17, 201-217.

Roos E., U. Eisele, H. Silcher and D. Kiessling (1987). Determination of J-Curves by Large Scale Specimen. 13-MPA Seminar, MPA Stuttgart, Germany.

Rousselier G., J.C. Devaux, G. Mottet and G. Devesa (1986). A methodology for ductile fracture analysis based on damage mechanics : an illustration of local approach of fracture. ASTM Third Non linear Fracture Mechanics Symposium, Knoxville, 6-8 October.

Rousselier G. (1987). Ductile fracture models and their potential in local approach of fracture. Nuclear Eng. and Design, 105, 97-111.